

Displacement damage effects on the p-GaN HEMT induced by neutrons at Back-n in the China Spallation Neutron Source

Yu-Fei Liu(刘宇飞), Li-Li Ding(丁李利), Yuan-Yuan Xue(薛院院), Shu-Xuan Zhang(张书瑄), Wei Chen(陈伟), and Yong-Tao Zhao(赵永涛)

Citation: Chin. Phys. B, 2025, 34 (**10**): 106102. DOI: 10.1088/1674-1056/addd80
http://cpb.iphy.ac.cn; http://iopscience.iop.org/cpb

What follows is a list of articles you may be interested in

A large-area scintillation neutron detector based on WLSF and SiPM readout

Xiao-Hu Wang(王小胡), Yang-Tu Lu(卢扬图), Bin Tang(唐彬), Xiu-Ku Wang(王修库), Shao-Jia Chen(陈少佳), Ze-Ren Li(李泽仁), and Zhi-Jia Sun(孙志嘉)

Chin. Phys. B, 2025, 34 (**6**): 066106. DOI: 10.1088/1674-1056/adcb1c

Analysis of displacement damage effects on the charge-coupled device induced by neutrons at Back-n in the China Spallation Neutron Source

Yuan-Yuan Xue(薛院院), Zu-Jun Wang(王祖军), Wei Chen(陈伟), Xiao-Qiang Guo(郭晓强), Zhi-Bin Yao(姚志斌), Bao-Ping He(何宝平), Xu Nie(聂栩), Shankun Lai(赖善坤), Gang Huang(黄港), Jiang-Kun Sheng(盛江坤), Wu-Ying Ma(马武英), and Shi-Long Gou(缑石龙)

Chin. Phys. B, 2023, 32 (**7**): 076101. DOI: 10.1088/1674-1056/acac07

Impact of incident direction on neutron-induced single-bit and multiple-cell upsets in 14 nm FinFET and 65 nm planar SRAMs

Shao-Hua Yang(杨少华), Zhan-Gang Zhang(张战刚), Zhi-Feng Lei(雷志锋), Yun Huang(黄云), Kai Xi(习凯), Song-Lin Wang(王松林), Tian-Jiao Liang(梁天骄), Teng Tong(童腾), Xiao-Hui Li(李晓辉), Chao Peng(彭超), Fu-Gen Wu(吴福根), and Bin Li(李斌)

Chin. Phys. B, 2022, 31 (**12**): 126103. DOI: 10.1088/1674-1056/ac785a

Effect of heavy ion irradiation on the interface traps of AlGaN/GaN high electron mobility transistors

Zheng-Zhao Lin(林正兆), Ling Lü(吕玲), Xue-Feng Zheng(郑雪峰), Yan-Rong Cao(曹艳荣), Pei-Pei Hu(胡培培), Xin Fang(房鑫), and Xiao-Hua Ma(马晓华)

Chin. Phys. B, 2022, 31 (**3**): 036103. DOI: 10.1088/1674-1056/ac11e4

First neutron Bragg-edge imaging experimental results at CSNS

Jie Chen(陈洁), Zhijian Tan(谭志坚), Weiqiang Liu(刘玮强), Sihao Deng(邓司浩), Shengxiang Wang(王声翔), Liyi Wang(王立毅), Haibiao Zheng(郑海彪), Huaile Lu(卢怀乐), Feiran Shen(沈斐然), Jiazheng Hao(郝嘉政), Xiaojuan Zhou(周晓娟), Jianrong Zhou(周健荣), Zhijia Sun(孙志嘉), Lunhua He(何伦华), and Tianjiao Liang(梁天骄)

Chin. Phys. B, 2021, 30 (**9**): 096106. DOI: 10.1088/1674-1056/ac0da7

Displacement damage effects on the p-GaN HEMT induced by neutrons at Back-n in the China Spallation Neutron Source

Yu-Fei Liu(刘宇飞)[1], Li-Li Ding(丁李利)[2], Yuan-Yuan Xue(薛院院)[2,3], Shu-Xuan Zhang(张书瑄)[1], Wei Chen(陈伟)[2,†], and Yong-Tao Zhao(赵永涛)[1,‡]

[1] *MOE Key Laboratory for Nonequilibrium Synthesis and Modulation of Condensed Matter, School of Physics, Xi'an Jiaotong University, Xi'an* 710049, *China*

[2] *National Key Laboratory of Intense Pulsed Radiation Simulation and Effect, Xi'an* 710024, *China*

[3] *State Key Laboratory of Artificial Microstructure and Mesoscopic Physics, School of Physics, Peking University, Beijing* 100871, *China*

(Received 2 February 2025; revised manuscript received 13 May 2025; accepted manuscript online 28 May 2025)

Irradiation experiments on p-GaN gate high-electron-mobility transistors (HEMTs) were conducted using neutrons at Back-streaming White Neutron (Back-n) facility at the China Spallation Neutron Source (CSNS). Two groups of devices were float-biased, while one group was ON-biased. Post-irradiation analysis revealed that the electrical performance of the devices exhibited progressive degradation with increasing Back-n fluence, with the ON-biased group demonstrating the most pronounced deterioration. This degradation was primarily characterized by a negative shift in the threshold voltage, a significant increase in reverse gate leakage current, and a slight reduction in forward gate leakage. Further analysis of the gate leakage current and capacitance–voltage characteristics indicated an elevated concentration of two-dimensional electron gas (2DEG), attributed to donor-type defects introduced within the barrier layer by Back-n irradiation. These defects act as hole traps, converting into fixed positive charges that deepen the quantum-well conduction band, thereby enhancing the 2DEG density. Additionally, through the trap-assisted tunneling mechanism, these defects serve as tunneling centers, increasing the probability of electron tunneling and consequently elevating the reverse gate leakage current.

Keywords: displacement damage effects, HEMT, Back-n, CSNS, threshold voltage shift

PACS: 61.80.Hg, 71.55.Eq, 73.40.Kp

DOI: 10.1088/1674-1056/addd80 **CSTR:** 32038.14.CPB.addd80

1. Introduction

GaN-based AlGaN/GaN high-electron-mobility transistors (HEMTs) have a wide range of applications in space.[1–3] However, exposure to various complex particles in space can lead to different radiation effects that may affect their performance.[4–10] Among the three primary irradiation effects, the displacement damage effect is particularly significant and frequently occurs in HEMT devices.[11,12] Neutrons and protons can induce displacement damage in these devices, creating traps, and leading to performance degradation.[13–17]

Numerous studies have investigated the radiation effects on p-GaN HEMTs. For instance, Wan *et al.*[18] conducted low-energy proton irradiation experiments on commercial p-GaN HEMTs and observed a negative shift in the threshold voltage ($V_{\rm th}$). Their results suggest that low-energy proton radiation introduces numerous charged donor traps within the device, which can capture electrons, scatter carriers, or partially compensate for p-type doping in p-GaN. Meanwhile, Wu *et al.*[19] explored the total-dose effect of p-GaN HEMTs and found that irradiation alters the competition between electron trapping at the metal/p-GaN interface and hole injection at the p-GaN/AlGaN interface, thereby determining the eventual $V_{\rm th}$ shift. Additionally, Lv *et al.*[20] performed 1 MeV neutron irradiation experiments at a fluence of 1×10^{15} cm^{-2} and reported a significant increase in gate leakage current, accompanied by a slight positive shift in $V_{\rm th}$. In contrast, Bôas *et al.*[21] observed a 0.2 V negative shift in $V_{\rm th}$ following irradiation with 14 MeV neutrons, which diverged from the findings of previous experiments. Despite the simplicity and controllability of p-GaN gate technology, research on its radiation effects and reliability remains limited due to its relatively recent development. Back-n radiation, which can simulate high-altitude atmospheric neutron environments, offers a valuable tool for evaluating the radiation reliability of HEMTs. However, no prior studies have investigated the effects of Back-n radiation on p-GaN HEMTs. Therefore, conducting such research is essential to advance our understanding of the radiation-induced degradation mechanisms in these devices and to ensure their reliability in radiation environments.

To investigate the displacement damage of enhanced HEMT devices by Back-n, this paper presents irradiation experiments on commercial 650 V p-GaN enhanced HEMT devices. This experiment was conducted at the Bank-n in the CSNS to systematically evaluate the degradation of electrical

†Corresponding author. E-mail: chenwei@nint.ac.cn

‡Corresponding author. E-mail: zhaoyongtao@xjtu.edu.cn

© 2025 Chinese Physical Society and IOP Publishing Ltd. All rights, including for text and data mining, AI training, and similar technologies, are reserved.

properties. We employed gate leakage current measurements, capacitance–voltage (C–V) curve characterization, and technology computer-aided design (TCAD) simulations to explore damage mechanisms.

2. Experimental details

2.1. Device under test (DUT)

The p-GaN HEMTs used in this study as experimental samples are sourced from Infineon. The device is a 650 V p-GaN HEMTs with an on-resistance of 100 mΩ and a maximum leakage current of 15 A. To minimize device-related variability, 6 HEMTs with comparable performance were selected as sample devices. The schematic diagram and optical image of the p-GaN HEMTs are presented in Fig. 1.

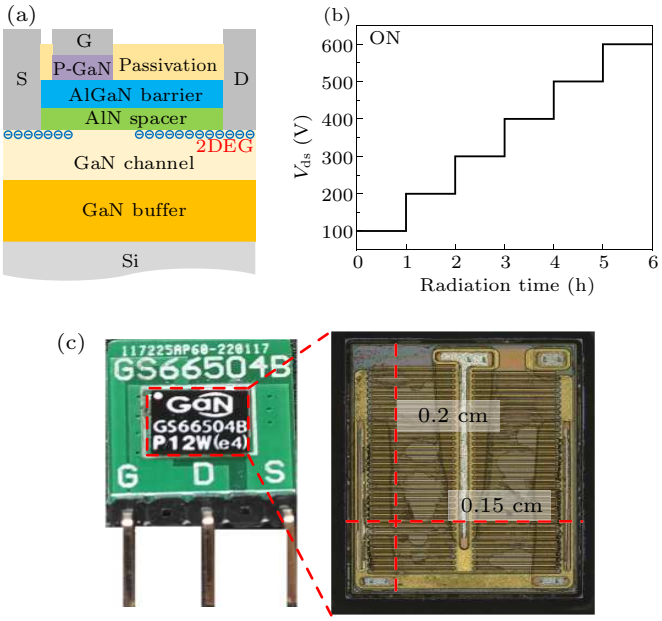


Fig. 1. (a) Schematic diagram of the p-GaN enhanced AlGaN/GaN HEMT device. (b) ON bias set of the AlGaN/GaN HEMT device irradiation experiment. (c) Optical image of the p-GaN HEMT.

2.2. Experimental setup

Neutron displacement damage experiments were conducted at the CSNS, the fluence of Back-n is 2.6×10^7 n/(cm^2·s). We selected three sets of p-GaN HEMTs with comparable performance, as shown in Fig. 2. Experiments were carried out at three different neutron fluences: 1.5×10^{11} n/cm^2, 4.5×10^{11} n/cm^2, and 6.5×10^{11} n/cm^2. Notably, the device for fluence of 4.5×10^{11} n/cm^2 is under ON bias and a drain voltage is applied, as shown in Fig. 1(b). Electrical performance tests were carried out using an Agilent B1500 semiconductor parameter analyzer. These tests primarily included transfer characteristics, gate leakage, and capacitance performance, which are essential for subsequent degradation analysis and calculations.

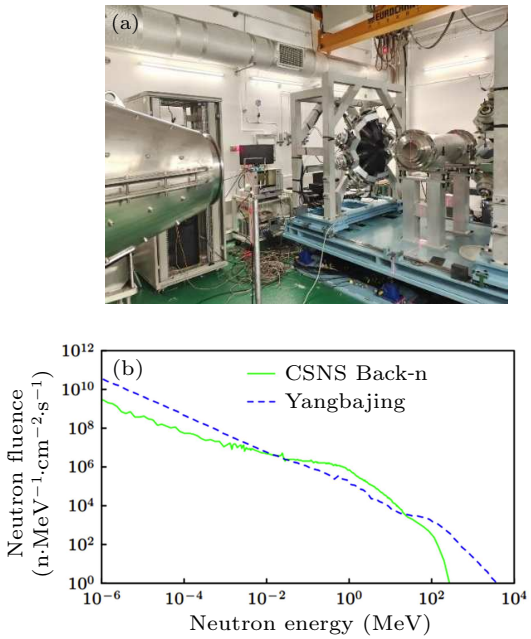


Fig. 2. (a) Image of the experimental setup at Back-n in the CSNS. (b) The energy spectrum of Back-n and Yangbajing.[22]

3. Experimental result

The transfer characteristics and gate leakage characteristics curves of the DUTs, both before and after irradiation, are shown in Fig. 3 under different neutron radiation fluences. We define V_{gs} at $V_{ds} = 1$ V and $I_d = 1$ mA as the threshold voltage (V_{th}); I_g at $V_{ds} = 0$ V and $V_{gs} = -10$ V as the reverse gate leakage; and I_g at $V_{ds} = 0$ V and $V_{gs} = 2$ V as the forward gate leakage.[23]

From Figs. 3(a) and 3(c), it is evident that V_{th} gradually shifts negatively with the increase in neutron fluence. Meanwhile, the reverse gate leakage current rises, while the forward gate leakage current experiences a slight decrease, as illustrated in Figs. 3(b) and 3(d). At the fluence of 1.5×10^{11} n/cm^2, the V_{th} of the device remains relatively stable, while the reverse gate leakage current exhibits significant degradation.

In contrast, at a fluence of 6.5×10^{11} n/cm^2, there is a negative shift in the V_{th}, accompanied by only a minor change in the reverse gate leakage current. This indicates that the degradation caused by irradiation results from multiple factors. As can be seen from Figs. 3(e) and 3(f), the performance degradation of the device in the ON-bias state is more pronounced, exhibiting a more significant negative shift in V_{th} and a larger change in reverse gate leakage. The ON-bias experimental results indicate that the device is more sensitive to neutron irradiation when in the ON state, leading to more significant performance degradation. This is because the bias voltage under ON bias increases the energy of the recoil nucleus,[24] which in turn contributes to defect generation and more severe degradation of the device.

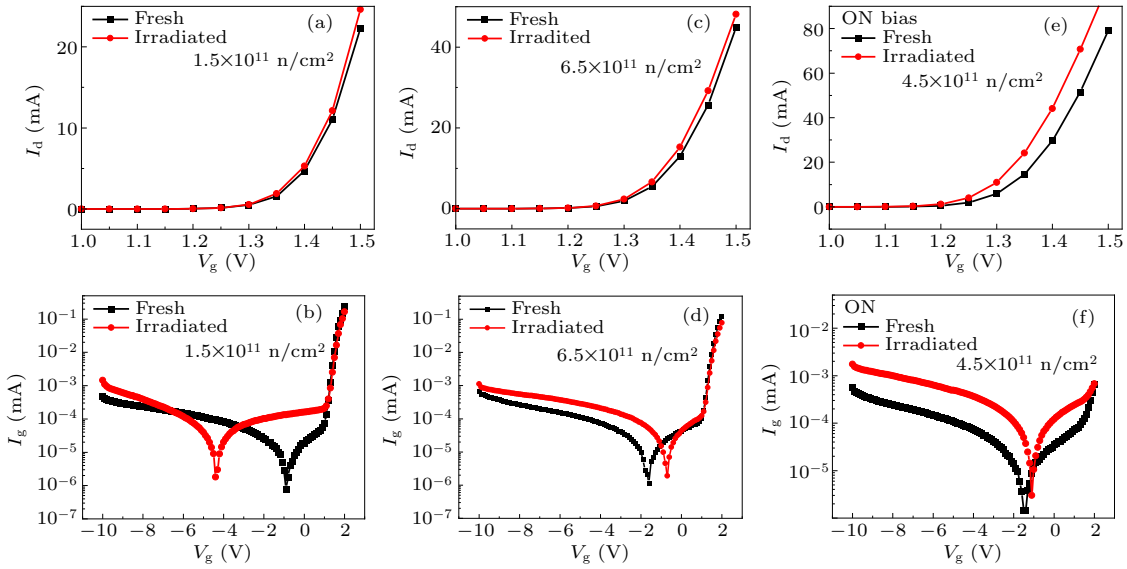


Fig. 3. Transfer characteristics and gate leakage current of the DUTs. Neutron radiation fluence: (a), (b) 1.5×10^{11} n/cm^2, (c), (d) 6.5×10^{11} n/cm^2, (e), (f) 4.5×10^{11} n/cm^2 under ON bias.

4. Analysis and discussion

4.1. Gate leakage current

Gate leakage current can be mainly divided into thermionic emission and tunneling current. By analyzing and calculating the gate leakage curve, the percentage of tunneling current can be determined, allowing for an assessment of the changes of defects within the barrier layer.[17] The linear portion of the forward gate leakage curve, as shown in Fig. 4, was extracted and fitted according to[20]

$$\ln J = \frac{q}{nkT}V_{\rm g} + \ln AA^*T^2 - \frac{q\phi_{\rm b}}{kT}. \tag{1}$$

Here $A^* = 4\pi qk^2m^*/h^3$ is Richardson's constant, A is the area, $\phi_{\rm b}$ is the Schottky barrier height, n is the ideality factor, and T is the temperature.

The Schottky barrier and the ideal factor were calculated, and the results are presented in Table 1. It is evident that the Schottky barrier progressively increases with rising neutron fluence, while the ideal factor also continues to increase. The degradation is most significant for DUTs under ON bias, where the Schottky barrier increases by 0.004 eV and the ideal factor rises by 107%. The nonlinear behavior of the fitted curves primarily results from a current transport mechanism other than thermionic emission, which is typically attributed to tunneling current caused by defects in the barrier layer. The increase in the ideality factor indicates an increasing proportion of tunneling currents, suggesting that the defect density within the barrier layer is increasing. From Table 1, prior to irradiation, the Schottky barrier and ideality factor of the device under ON bias are higher than those of the other groups. This indicates that the density of donor-like defects beneath the p-GaN layer of the HEMT under ON bias is greater. Given that the performance of HEMTs is influenced by various factors,[4] we speculate that the device may also possess acceptor-like defects with higher density or deeper energy levels in other regions. The competition between these two types of defects results in comparable performance of the HEMT relative to the others, which is discussed in Subsection 4.2.

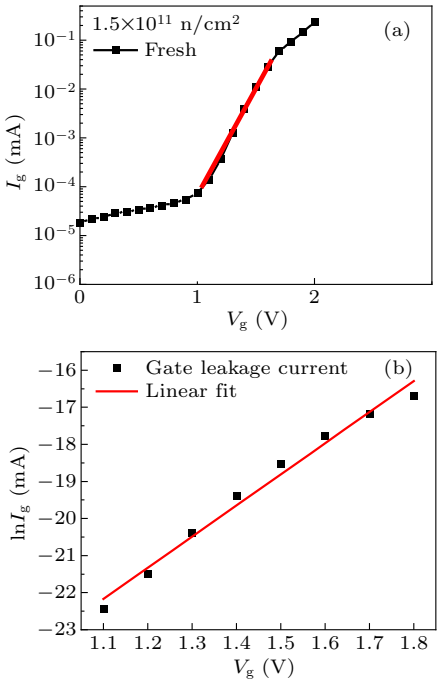


Fig. 4. (a) Forward gate leakage current. (b) Linear part of forward gate leakage for calculation.

Table 1. Schottky barrier and ideality factor before and after neutron irradiation.

Neutron fluence	Schottky barrier (eV)		Ideality factor	
	Fresh	Irradiated	Fresh	Irradiated
1.5×10^{11}	0.2049	0.206	1.73191	1.95935
6.5×10^{11}	0.20629	0.20744	1.99664	2.35828
4.5×10^{11}	0.20861	0.21243	4.43282	9.20378

4.2. Frequency-dependent admittance analysis

The *C*–*V* characteristic curve of the device illustrates the accumulation of electrons in the channel. Consequently, parameters such as defect density and energy levels at the heterojunction interface can be derived from the *C*–*V* curves through frequency-dependent admittance analysis. From Eqs. (2) and (3),[25] we will analyze the state of the defects in the channel layer by employing the measured *C*–*V* and capacitance-frequency (*C*–*f*) curves:

$$\frac{G_\mathrm{p}}{\omega} = \frac{\omega G_\mathrm{m} C_\mathrm{ac}^2}{G_\mathrm{m}^2 + \omega(C_\mathrm{ac} - C_\mathrm{m})}, \tag{2}$$

$$\frac{G_\mathrm{p}}{\omega} = \frac{qD_\mathrm{t}}{2\omega\tau_\mathrm{t}} \ln[1 + (\omega\tau_\mathrm{t})^2]. \tag{3}$$

Here, C_m and G_m are the measured values of the capacitance and the conductance, G_p is the equivalent capacitance, C_ac is the capacitance under the gate, $\omega = 2\pi f$, and τ_t and D_t are the relaxation time constant and density of defects.

Taking the calculation at $V_\mathrm{gs} = 1$ V as an example, the *C*–*V* and the *C*–*f* curves are tested at different frequencies. The values of G_m, C_ac, and C_m are extracted from the curves. Subsequently, the values of G_p/ω at different frequencies are calculated according to Eq. (1), as shown in the scatter plot in Fig. 5. Finally, the scatter plot is fitted nonlinearly using Eq. (2), and the fitted curve is shown in Fig. 5. The time constant, density, and energy level of the defects at the heterojunction interface are calculated from the parameter values of the fitted curves.

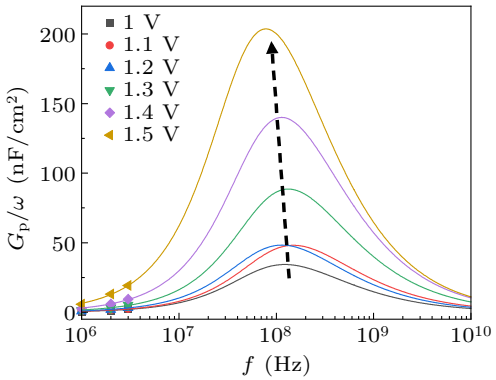


Fig. 5. The calculation of the DUT by frequency-dependent admittance analysis before irradiation. The frequency of the peak point on the fitted curve decreases with increasing voltage.

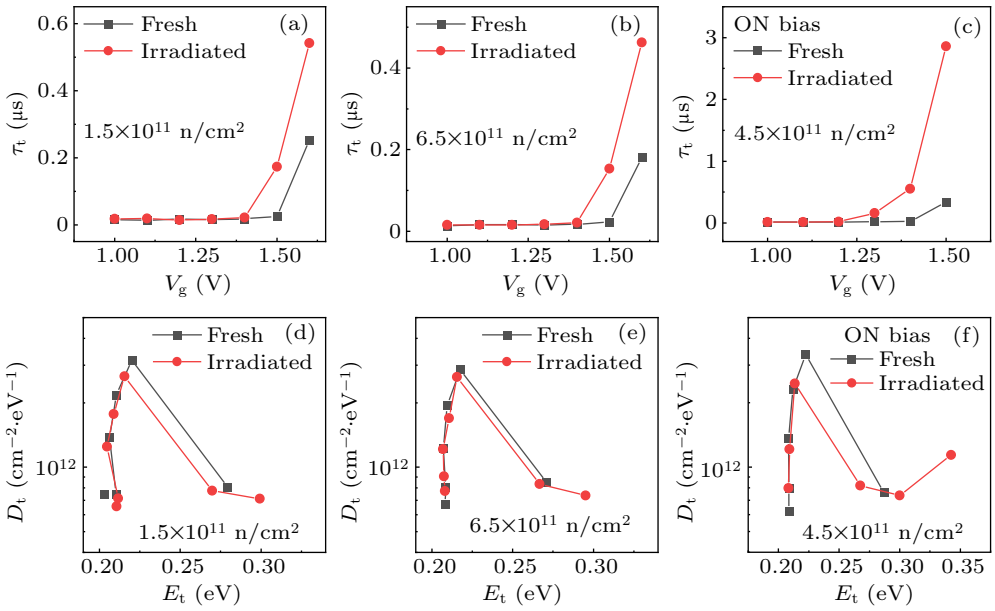


Fig. 6. Relaxation time constant for (a) 1.5×10^{11} n/cm^2, (b) 6.5×10^{11} n/cm^2 and (c) 4.5×10^{11} n/cm^2 under ON bias. Trap concentration at heterojunction for (d) 1.5×10^{11} n/cm^2, (e) 6.5×10^{11} n/cm^2 and (f) 4.5×10^{11} n/cm^2 under ON bias.

As shown in Fig. 6, the time constants of the defects at the heterojunction interfaces generally increase, and the energy levels tend to deepen following irradiation, with only minor changes in defect densities. Notably, when comparing irradiation with the fluence of 1.5×10^{11} n/cm^2, the increase of fluence does not lead to a further rise in defect concentration or energy level at the heterojunction. This suggests that Back-n irradiation is less likely to generate deep energy level defects at the heterojunction. However, the higher fluence continues to generate donor defects in the barrier layer, leading to a larger negative V_th shift. The significantly deeper defect energy level under ON-bias conditions indicates that the device is more sensitive to irradiation under the ON bias. As shown in the calculations presented in Subsection 4.1, there are also many defects in the barrier layer, resulting in a more negative V_th shift.

4.3. TCAD

The calculations in Subsection 4.1 show that Back-n irradiation has created new defects in the barrier layer. According

to the literature, the neutron irradiation process not only generates acceptor defects at the heterojunction interface but also generates donor defects within the barrier layer. These defects contribute to an increase in gate leakage current through the trap-assisted tunneling effect.

Post-device modeling, guided by the findings in Subsection 4.1, we introduced varying concentrations of donor-type defects into the barrier layer to simulate the effects of different bias conditions. Given that the HEMT's ideality factor growth rate under ON bias is ten times higher than under OFF bias, we added defect concentrations of 1×10^{16} n/(cm^3·eV) and 1×10^{15} n/(cm^3·eV) to represent ON and OFF bias conditions, respectively. These specific concentrations were chosen to accurately reflect the impact of bias conditions on defect generation and to facilitate a direct comparison of their effects on HEMT performance. As shown in Fig. 7, we analyzed the effect of different density of defects in the barrier layer on the 2DEG density. Figures 7(a), 7(b), and 7(c) represent the fresh device, the device under OFF bias, and the device under ON bias, respectively.

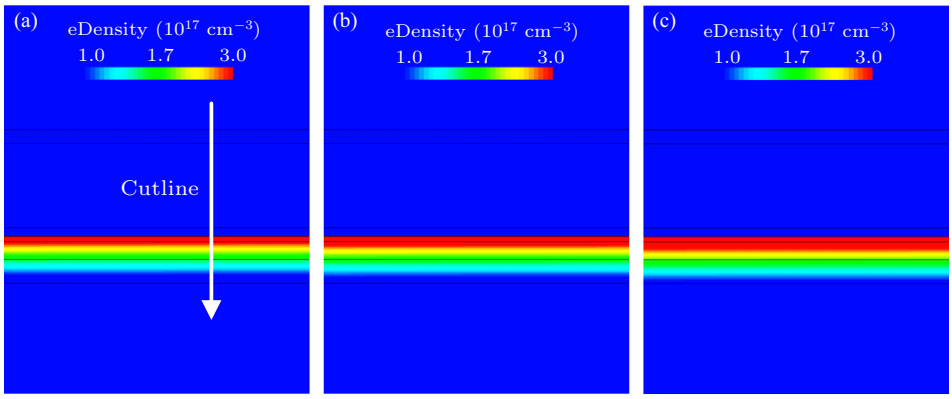


Fig. 7. The 2DEG density in TCAD model for (a) the fresh device, (b) OFF bias state, and (c) ON bias state.

The 2DEG of HEMT is generated by a polarization effect and is influenced by various factors. The calculation formula is shown in Eq. (4). Furthermore, $V_{\rm th}$ is calculated based on the concentration of 2DEG, as shown in Eq. (5):[26–28]

$$n_{\rm s}(x) = \frac{\sigma(x)}{e} - \frac{\varepsilon_0\varepsilon(x)}{e^2 d}(e\Phi_{\rm B}(x) - eV_{\rm g} + \Delta E_{\rm F}(x) - \Delta E_{\rm C}(x)), \tag{4}$$

$$V_{\rm th} = -\frac{\sigma(x)d}{\varepsilon_0\varepsilon(x)} + \Phi_{\rm B} + \frac{\Delta E_{\rm F}(x) - \Delta E_{\rm C}(x)}{e}. \tag{5}$$

Here, e is the electron charge, $\sigma(x)$ is the polarization charge density, d is the thickness of the AlGaN barrier layer, $\varepsilon_0\varepsilon(x)$ is the dielectric constant of the material, $e\phi_{\rm B}(x)$ is the height of the gate Schottky barrier, $\Delta E_{\rm F}(x)$ is the distance from the bottom of the conduction band of the GaN quantum well to the Fermi level, and $\Delta E_{\rm C}(x)$ is the difference in height between the AlGaN conduction band and the GaN conduction band.

The conduction band energy levels and 2DEG density changes along the cutline were extracted in Figs. 8(a) and 8(b). As the defect density increases, the conduction band of the device becomes deeper and the 2DEG density increases.

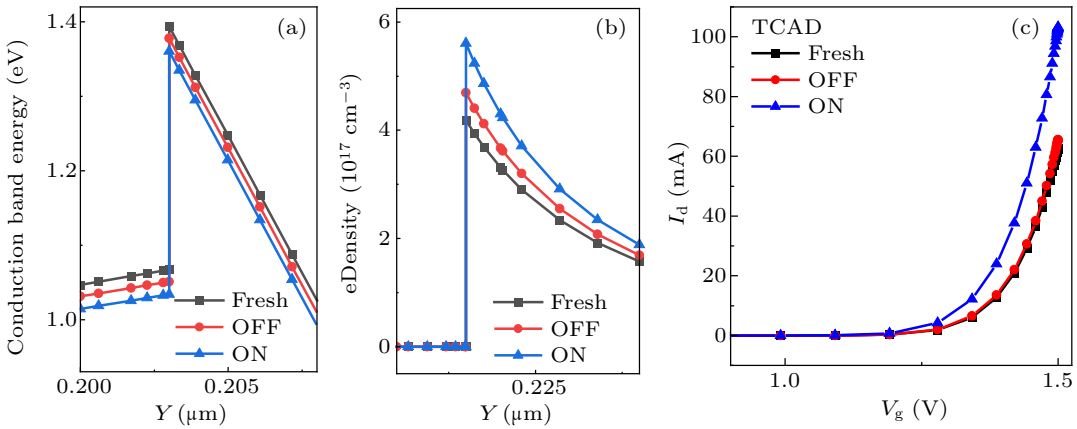
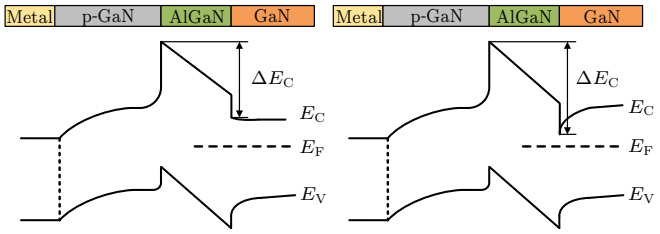


Fig. 8. (a) Conduction band energy and (b) 2DEG density along the section line in the TCAD model. (c) Transfer characteristics in TCAD.

The 2DEG of GaN HEMTs is generated through the polarization effect. In this process, the conduction band of the heterojunction lies below the Fermi energy level, resulting in the accumulation of electrons that form the 2DEG. The holes generated by radiation may be captured by the defects in the barrier layer, forming a fixed positive charge or deep level

traps. It will also lower the conduction band height at the channel, resulting in an increase in $\Delta E_C(x)$. This deepening of the conduction band and increase in $\Delta E_C(x)$ increases the concentration of the 2DEG, which is the primary reason for the negative V_{th} shift, as shown in Fig. 9.



(a) Pre-irradiation (b) Post-irradiation

Fig. 9. The comparison of band structures of the p-GaN HEMT during radiation. (a) Pre-irradiation, (b) post-irradiation. This reveals the degradation mechanism of the HEMTs.

5. Conclusion

In this paper, we present the results of Back-n irradiation experiments conducted on p-GaN gate HEMTs at the CSNS with three different neutron fluences. The results indicate that the V_{th} of the HEMT devices gradually shifts negatively as neutron fluence increases. Additionally, we observe an increase in reverse gate leakage, while forward gate leakage experiences a slight decrease. Analysis of the gate leakage curves suggests that the Back-n irradiation introduces new donor defects within the barrier layer. These defects act as tunneling centers, increasing the tunneling probability, which contributes to the rise in reverse gate leakage. The analysis of defects at heterojunction interfaces using the variable frequency conduction method revealed that the energy levels of these defects gradually deepen during irradiation, which results in the trapping of 2DEG. However, this change is minor and has little impact on performance. Subsequently, TCAD simulations revealed that the defects within the barrier layer led to a decrease in the conduction band, significantly increasing the 2DEG density and further contributing to the negative V_{th} shift.

Acknowledgements

Project supported by the National Natural Science Foundation of China (Grant Nos. 12120101005, U2030104, 12175174, 11975174, and 12105229), State Key Laboratory Foundation of Laser Interaction with Matter (Grant Nos. SKLLIM1807 and SKLLIM2106), the Postdoctoral Fellowship Program of CPSF (Grant No. GZC20241372), and National Key Laboratory of Intense Pulsed Radiation Simulation and Effect (Grant No. NKLIPR2419).

References

[1] Grant J, Cunningham W, Blue A, O'Shea V, Vaitkus J, Gaubas E and Rahman M 2005 *Nucl. Instr. Meth. A* **546** 213
[2] Kozak J P, Zhang R, Porter M, Song Q, Liu J, Wang B, Wang R, Saito W and Zhang Y 2023 *IEEE Trans. Power Electron.* **38** 8442
[3] Tsao J Y, Chowdhury S, Hollis M A, *et al.* 2018 *Adv. Elect. Materials* **4** 1600501
[4] Zhou X, Wang Z, Wu Z, Zhou Q, Qiao M, Li Z and Zhang B 2023 *IEEE Trans. Electron Devices* **70** 4081
[5] Bonaldo S, Zhang E X, Mattiazzo S, Paccagnella A, Gerardin S, Schrimpf R D and Fleetwood D M 2023 *IEEE Trans. Nucl. Sci.* **70** 2042
[6] Chen C, Tian B L, Liu X Z, Dai L P, Deng X W and Chen Y F 2012 *Chin. Phys. B* **21** 078503
[7] Wang Y P, Luo Y H, Wang W, Zhang K Y, Guo H X, Guo X Q and Wang Y M 2013 *Chin. Phys. C* **37** 056201
[8] Li Q, Lou H and Zhu L 2023 *Appl. Phys. A* **129** 374
[9] Yue S, Lei Z, Peng C, Zhong X, Wang J, Zhang Z, En Y, Wang Y and Hu L 2020 *IEEE Trans. Nucl. Sci.* **67** 1339
[10] Ives N E, Chen J, Witulski A F, Schrimpf R D, Fleetwood D M, Bruce R W, McCurdy M W, Zhang E X and Massengill L W 2015 *IEEE Trans. Nucl. Sci.* **62** 2417
[11] Martinez M J, King M P, Baca A G, Allerman A A, Armstrong A A, Klein B A, Douglas E A, Kaplar R J and Swanson S E 2019 *IEEE Trans. Nucl. Sci.* **66** 344
[12] Fleetwood D M, Zhang E X, Schrimpf R D and Pantelides S T 2022 *IEEE Trans. Nucl. Sci.* **69** 1105
[13] Berthet F, Petitdidier S, Guhel Y, Trolet J L, Mary P, Gaquiere C and Boudart B 2016 *IEEE Trans. Nucl. Sci.* **63** 1918
[14] Zhang M L, Wang X L, Xiao H L, Wang C M, Ran J X and Hu G X 2008 *Chin. Phys. Lett.* **25** 1045
[15] Polyakov A Y, Smirnov N B, Govorkov A V, Shlensky A A and Pearton S J 2004 *J. Appl. Phys.* **95** 5591
[16] Ahmed M, Kucukgok B, Yanguas-Gil A, Hryn J and Wender S A 2020 *Radiation Physics and Chemistry* **166** 108456
[17] Lv L, Yan X, Cao Y, Zhu Q, Yang L, Zhou X, Ma X and Hao Y 2019 *IEEE Trans. Nucl. Sci.* **66** 886
[18] Wan X, *et al.* 2017 *IEEE Trans. Nucl. Sci.* **64** 253
[19] Wu H, Fu X, Guo J, Liu T, Wang Y, Luo J, Huang Z and Hu S 2022 *IEEE Electron Device Lett.* **43** 1945
[20] Lü L, Zhang J C, Xue J S, Ma X H, Zhang W, Bi Z W, Zhang Y and Hao Y 2012 *Chin. Phys. B* **21** 037104
[21] Bôas A C V, *et al.* 2024 2024 *38th Symposium on Microelectronics Technology and Devices (SBMicro) Joao Pessoa*, Brazil, 2024-09-02 pp. 1–4
[22] Wang X, Zhang F Q, Chen W, Guo X Q, Ding L L and Luo Y H 2020 *Acta Phys. Sin.* **69** 162901 (in Chinese)
[23] Tang X, Li B, Moghadam H A, Tanner P, Han J and Dimitrijev S 2018 *IEEE Electron Device Lett.* **39** 1145
[24] Yue S, Wang Y, Zheng X, Pan A, Hong Y, Wang X, Gong S, Zhu T, Zhang F, Ma X and Hao Y 2024 *Appl. Phys. Lett.* **124** 122105
[25] Arslan E, Bütün S, Şafak Y and Ozbay E 2010 *J. Electron. Mater.* **39** 2681
[26] Aziz M A and El-Abd A 2006 *Proceedings of the Twenty Third National Radio Science Conference (NRSC'2006) Menouf*, Egypt, 2006 D6 1
[27] Rashmi, Kranti A, Haldar S and Gupta R S 2002 *Solid-State Electronics* **46** 621
[28] Krantz R J and Bloss W L 1989 *IEEE Trans. Electron Devices* **36** 451